Carbonic anhydrase IX inhibitor S4 triggers immunogenic cell death in glioma cells via endoplasmic reticulum stress pathway

Jing Cui
Cancer Hospital of China Medical University, Liaoning Cancer Hospital & Institute
Huizhe Xu
Cancer Hospital of China Medical University, Liaoning Cancer Hospital & Institute
Ji Shi
Cancer Hospital of China Medical University, Liaoning Cancer Hospital & Institute
Kun Fang
Dalian Medical University
Dapeng Liang
Dalian Medical University
Feng Liu
Cancer Hospital of China Medical University, Liaoning Cancer Hospital & Institute
Jing Wang
Dalian Medical University
Chunrui Xie
Dalian Medical University
Zhiyu Xia
Dalian Medical University
Songshu Meng (ssmeng@dmu.edu.cn)
Dalian Medical University
Yumei Yan
the First Affiliated Hospital to Dalian Medical University
Haozhe Piao
Cancer Hospital of China Medical University, Liaoning Cancer Hospital & Institute

---

Research Article

Keywords: Carbonic anhydrase IX inhibitor, immunogenic cell death, glioma, endoplasmic reticulum (ER) stress, S4

Posted Date: June 17th, 2022

DOI: https://doi.org/10.21203/rs.3.rs-1759379/v1

Abstract

Purpose: Immunogenic cell death (ICD), which releases danger-associated molecular patterns (DAMP) that induce potent anticancer immune response, has emerged as a key component of therapy-induced anti-tumor immunity. The aim of this work was to analyze whether the carbonic anhydrase IX inhibitor S4 can elicit ICD in glioma cells.

Methods: The effects of S4 on glioma cell growth were evaluated using the CCK-8, clonogenic and sphere assays. Glioma cell apoptosis was determined by flow cytometry. Surface-exposed calreticulin (CRT) was inspected by confocal imaging. The supernatants of S4-treated cells were concentrated for the determination of HMGB1and HSP70/90 expression by immunoblotting. RNA-seq was performed to compare gene expression profiles between S4-treated and control cells. Pharmacological inhibition of apoptosis, autophagy, necroptosis and endoplasmic reticulum (ER) stress was achieved by inhibitors. In vivo effects of S4 were evaluated in glioma xenografts. Immunohistochemistry (IHC) was performed to stain Ki67 and CRT.

Results: S4 significantly decreased the viability of glioma cells and induced apoptosis and autophagy. Moreover, S4 triggered CRT exposure and the release of HMGB1 and HSP70/90. Inhibition of either apoptosis or autophagy significantly reversed S4-induced release of DAMP molecules. RNA-seq analysis indicated that the ER stress pathway was deregulated upon exposure to S4. Both PERK-eIF2α and IRE1α-XBP1 axis were activated in S4-treated cells. Furthermore, pharmacological inhibition of PERK significantly suppressed S4-triggered ICD markers and autophagy. In glioma xerografts, S4 significantly reduced tumor growth.

Conclusions: Altogether, these findings suggest S4 as a novel ICD inducer in glioma and might have implications for S4-based immunotherapy.

Introduction

Gliomas are the most common type of primary intracranial tumors. Conventional therapies, including surgery, radiotherapy, and pharmacotherapy (typically chemotherapy with temozolomide), have not significantly improved the median survival of patients with malignant glioma [1]. Accumulating evidence reveals that some conventional treatments, in addition to their direct cytotoxic effect, could induce an antitumor immune response [2]. Immunogenic cell death (ICD), named after the immunogenicity of dying/dead cancer cells, is induced by certain types of therapies [3–4]. ICD has emerged as a key component of therapy-induced anti-tumor immunity [5]. Of note, some ICD inducers can function in synergy with other types of immunotherapy, such as immune checkpoint inhibitors therapy to potentiate their effectiveness [6]. ICD is characterized by the emission of immuno-stimulatory molecules, including damage-associated molecular patterns (DAMPs) such as cell surface exposure of the endoplasmic reticulum protein calreticulin, secretion of ATP, and release of the chromatin-binding protein HMGB1[3, 7]. Other DAMPs such as heat-shock proteins (HSP90 and HSP70) are also exposed on the outer membrane

of the dying cells or released[8–10]. These DAMP molecules play a key role in activating dendritic cells (DCs) to engulf dying tumor cells, to process and present released tumor antigens to T cells [11–13]. Given the therapeutic potential of ICD in several types of cancer, a few pre-clinical investigations have shown that malignant gliomas might benefit from ICD-based therapies [4].

Carbonic anhydrase IX (CAIX), a tumor-associated, cell-surface glycoprotein in response to hypoxia, plays a pivotal role in pH homeostasis, which is essential for tumor cell survival. Literature documents that CAIX is implicated in cancer progression [14–16], and has been validated as a promising new anticancer target [17]. Several CAIX inhibitors such as SLC-0111, have been developed and shown to be effective in reducing primary tumor growth in vitro and in vivo [18]. S4, a CAIX specific sulfamate inhibitor [19], exhibited anti-proliferative efficacy in breast and colorectal tumor cells [20–23]. In addition, an antimetastatic effect of S4 in breast carcinoma xenografts was reported [19]. Of interest, S4 has shown to potentiate the efficacy of standard treatment modalities, such as doxorubicin in breast cancer [24], cisplatin in small cell lung cancer [25], suggesting a S4-based combination strategy against tumors. However, whether S4 would suppress glioma growth has not been investigated.

In the present study, we examined the effect of treatment with S4 on glioma cell growth in cell cultural systems and in murine models of glioma. Our data demonstrate that S4 triggers ICD in glioma cells via the induction of ER stress pathway. These preliminary data could represent the basis for further studies in order to exploring a potential role of S4 as an ICD inducer for treatment of malignant glioma.

Materials And Methods

Cell Lines, Regents and Antibodies

Human glioma cell lines Hs683, LN229 and U87MG were obtained from the American Type Culture Collection (ATCC). The human astrocytes HA cell line was obtained from ScienCell. Hs683 and HA were cultured with DMEM which contained 10% FBS. LN229 were cultured with 5% FBS DMEM. U87MG was cultured with 10% FBS MEM EAGLE. All cells were maintained at 37°C in a humidified incubator with 5% CO_2. S4 was obtained from Tocris Bioscience. Mitoxantraone (MTX), Necrostain-1, Z-VAD-FMK, 4μ8C were purchased from SELLECK. GSK2606414 was purchased from Apexbio, ISRIB was purchased from MCE. Chloroquine (CQ) was obtained from Sigma. 4', 6-diamidino-2-phenylindole (DAPI) was purchased from Beyotime; Pierce®Protein Concentrator PES and 10K MWCO were purchased from Thermo Fisher Scientific.

The following antibodies were used: HMGB1 (A2553, Abclonal, USA), Calreticulin (ab2907, abcam, UK) and HSP70 (ab2787, abcam, UK), GAPDH (10494-1-AP, Proteintech Technology, USA), Anti-Rabbit Alexa488 (A-11070, Invitrogen, USA), pIRE1α (NB100-2323, Novus, USA), LC3 (Ml52-3, MBL, Japan). The following antibodies were purchased from Cell Signaling Technology (USA): ATF4 (11815S), HSP90 (4874S), IRE1α (3294S), PARP (9532S), p-PERK (3179S), PERK (5683S), p-eIF2α (9721S), P62 (16177S), RIP(4920S), RIP3 (13526S), XBP-1s (12782S).

Cell Counting kit-8 assay

Cells were cultured in a 96-well plate with a density of 2000 cells per well, and were incubated with varying drug (S4) concentrations (0.01, 0.1, 1, 10 and 100 μM) for 24, 48, 72 h respectively. CCk-8 was incubated at 37°C for 1 to 4 hours per well. The absorbance value of cells in each well was detected at 450nm with a multifunctional microplate reader.

Colony formation assay

Cells were cultured in 6-well plates at a density of 2000/ well, and treated with 60 μM S4 or 0.05% DMSO. After 2 weeks, cells were fixed with 4% paraformaldehyde and stained with crystal violet for 20 minutes. The formation of cell clones were examined and taken photos for statistics.

Spheroid formation assay

Glioma cells were plated at (1×10^3/well) in ultra-low adhesion 96-well plates, incubating with serum-deprived DMEM/F12 medium containing 20 ng/ml basic FGF, 20 ng/mL of EGF, and a proportion of B27 in medium(1:50 v/v) for 10–14 days.

Immunofluorescence assay

Glioma cells were seeded on coverslips (NEST, 801008) for 12 h, then treated with drugs according to the purpose of the experiment. Then cells were fixed in 4% paraformaldehyde (PFA). After the blocking in 2% Bovine Serum Albumin (BSA), cells were then incubated with primary antibody (Calreticulin, 1: 75) for 2 h at room temperature, followed by 30 min incubation with secondary antibodies (Anti-Rabbit Alexa488, 1: 1000) at room temperature. Nuclei were stained with 1 μg/mL DAPI (C1002, Beyotime, China) in PBS. A laser scanning confocal microscope (Leica TCS SP5) was applied to monitor the immunofluorescence (IF).

Preparation of Concentrated Supernatants

The supernatants (5 ml) of S4-treated or DMSO-treated cells were collected and concentrated to 100 μl using Pierce®Protein Concentrator 2–6 ml/10K filters, according to the manufacturer's instructions.

Flow cytometric analysis of cell death

Glioma cells were treated with vehicle or S4 and stained with annexin V-FITC and propidium iodide (PI). Cells were subjected to flow cytometric analysis of membrane redistribution of phosphatidylserine. The percentage of apoptotic cells was determined in two independent experiments.

Immunoblotting

Cells were treated with various agents, collected and processed for immunoblotting analysis as previously described [26]. To quantify changes, the densitometries of protein bands were determined with a calibrated GS-670 densitometer.

RNA- sequencing

RNA was extracted from S4-treated and vehicle-treated LN229 cells and RNA- sequencing (RNA-seq) was performed by the Novogene Corporation (Beijing, China). RNA-seq data were analyzed as previously described [26]. RNA-seq data have been deposited at the NCBI Gene Expression Omnibus under the accession number GSE205538.

In vivo tumor xenograft experiment

LN229 cells (1×10^7) were injected subcutaneously into flanks of female BALB/c nude mice (6 weeks old), which were maintained in animal care facilities without specific pathogens. The mice were randomly divided into three groups (n = 5), namely, DMSO-treated, S4 at 10mg/kg, S4 at 50 mg/kg. Tumor growth was monitored using calipers where two perpendicular tumor diameters were measured every 5 days and tumor volume was calculated according to the formula $0.5 \times \text{length} \times \text{width}^2$. After 8 weeks, the tumor-bearing mice were sacrificed with ether anesthesia, and xenografts were excised.

Statistical analysis

SPSS 16.0 software was used for statistical data analysis. T-test or one-way ANOVA was used for comparison between groups. 0.05 was considered that the difference was statistically significant. The graphs were drawn using GrapPad Prism8.0.

Results

S4 decreases glioma cell viability

We assessed the effect of S4 on the viability of glioma cell lines Hs683, LN229, U87MG and human astrocytes HA cell line by a CCK-8 assay. As shown in (Fig. 1A), S4 inhibited the growth of the three glioma cell lines in both dose- and time- dependent manner. This effect was achieved with a much lower half maximal inhibitory concentrations (IC_{50}) values for glioma cell lines at each time point than the IC_{50} values for HA cells. Clonogenic growth assays showed that S4 at 60 μM decreased significantly the capability of the glioma cells to grow clonally after a 2-week treatment (Fig. 1B). Three-dimensional (3D) spheroid formation assays indicated that the LN2299 and U87MG microspheroids were substantially lessened in number after 10 days treatment with S4 (Fig. 1C). In addition, 24-hour S4 treatment caused a significant decrease in Ki67 staining in both LN229 and U87MG cells (Fig. 1D). Cumulatively, we showed that S4 decreases the viability of glioma cells in vitro.

S4 induces glioma cell death

We next determined whether the suppressed S4-induced growth inhibition in glioma cells was due to cell death. To this end, S4-treated LN229 and U87MG cells were analyzed by flow cytometry with FITC-conjugated Annexin-V and propidium iodide (PI) double staining. As illustrated in (Fig. 2A), exposure to S4 at 60 and 90 μM for 24 h significantly increased the percentage of both early and late apoptotic cells in LN229 and U87MG cell lines, suggesting an induction of apoptotic cell death. Doxorubicin (Dox) was used a positive control, which substantially increased the number of apoptotic cells as expected. In

addition, we observed large amounts of the cells from S4-treated spheroids derived from glioma cells were stained with the cell-death dye PI, indicative of cell death (Fig. 2B). Furthermore, a dose-dependent cleavage of Poly (ADP-ribose) polymerase (PARP), a classical apoptosis marker, was detectable in S4-treated glioma cells (Fig. 2C). In addition, we also detected an increase in microtubule-associated protein 1 light chain 3 (LC3)-II (an autophagy marker) levels in glioma cells upon exposure to S4, suggesting that S4 might induce autophagy in these cells. No obvious change in the levels of RIP1/3, two key proteins involved in necrosis, was detected in S4-treated glioma cells (Fig. 2D).

S4 induces CRT exposure and release of HMGB1 and HSP70/90 in glioma cells

We next investigated whether S4 could trigger ICD in glioma cells by examining the ICD markers including HMGB1and HSP70/90 in cellular supernatants and CRT expression (ecto-CRT) in cell surface. Mitoxantrine (MTX), a known ICD inducer [27], was chosen as a positive control. As illustrated in (Fig. 3A), confocal imaging of S4-treated LN229 and U87MG cells revealed a significantly increased exposure of CRT on the cell surface compared with DMSO-treated cells. As expected, MTX treatment induced a strong exposure of CRT in both glioma cell lines. To detect the secreted DAMPs such as HMGB1 and HSP70/90 in S4-treated glioma cells, the cell culture media was collected after a 24 h exposure to S4 and concentrated supernatants were assayed by immunoblotting. As depicted in (Fig. 3B), a robust increase in protein levels of both HMGB1 and HSP70/90 was detected in concentrated supernatants of S4-treated LN229 and U87MG cells. The above findings indicated that S4 might trigger ICD in glioma cells. Given that the incidence of ICD is generally acknowledged to be tightly connected with programmed cell death such as apoptosis, autophagy and necroptosis [28–30], we then tested whether apoptosis, autophagy and necroptosis would play a role in S4-triggered ICD. To this purpose, we pretreated the cells with an autophagy inhibitor chloroquine (CQ), a necroptosis inhibitor Necrostain-1 (Nec-1), and a pan-caspase inhibitor Z-VAD-FMK (Z-VAD), respectively. The effective concentrations of these inhibitors were selected by a dose–response assay for each compound to prevent cytotoxicity (data not shown). (Fig. 3C) shows that both CQ and Z-VAD-FMK substantially blocked the release of HMGB1 and HSP70/90 in LN229 and U87MG cells upon exposure to S4, while Nec-1could not exhibit similar effects. Moreover, S4-induced translocation of CRT on cell surface in glioma cells was significantly attenuated by pretreatment with either CQ or Z-VAD-FMK, but not Nec-1 (Fig. 3D).

ER stress pathway is involved in S4-mediated immunogenic cell death

To explore the signaling pathways involved in S4-mediated ICD in glioma cells, we performed RNA sequencing (RNA-seq) analysis to compare gene expression profiles between S4-treated LN229 cells and cells treated with vehicle. The gene ontology analysis demonstrated that the differentially expressed genes regulated by S4 were largely enriched in ER stress and unfolded protein response (UPR) pathways (Fig. 4A), suggesting a role for the ER stress pathway in S4-mediated ICD. To validate this, we examined the activation of PRKR-like endoplasmic reticulum kinase (PERK)-eIF2α axis, and inositol-requiring enzyme 1 alpha (IRE1α)-X-box binding protein 1 (XBP1) axis, two major upstream players in ER stress pathways. S4 treatment caused a substantial increase in the levels of XBP1 and the phosphorylated

eIF2α in both LN229 and U87MG cells (Fig. 4B), confirming an induction of ER stress pathway. To ascertain the role of ER stress pathway in S4-mediaed ICD, glioma cells were pre-incubated with ER stress pathway inhibitors GSK2606414 and ISRIB (both targeting PERK), and 4μ8C (targeting IRE1α) following S4 treatment. As shown in (Fig. 4C), pre-treatment of LN229 and U87MG cells with either GSK2606414 or ISRIB substantially reversed S4-induced secretion and release of HMGB1 and HSP70/90 while 4μ8C failed to do so, suggesting that the PERK-eIF2α axis plays a major role in S4-mediated ICD. Consistently, pre-exposure to GSK2606414 in LN229 cells or ISRIB in U87MG cells significantly blunted the translocation of CRT on cell surface induced by S4 (Fig. 4D). In addition, both GSK2606414 and ISRIB markedly reduced S4-induced LC3II expression in either LN229 or U87MG cells (Fig. 4E, **upper panels**). In addition, S4-iduced cleaved PARP was not affected by either GSK2606414 or ISRIB (Fig. 4E, **lower panels**). Altogether, these data suggest that these PERK inhibitors might antagonize S4-induced autophagy in the tested glioma cells.

S4 reduces glioma growth in mice models

To examine the effects of S4 in vivo, mice with LN229-derived tumors were injected with S4 at two different doses (10mg/kg and 50mg/kg). As illustrated in (Fig. 5A), both dose of S4 significantly reduced tumor growth without notable toxicity, while treatment with 50mg/kg dose of S4 achieved stronger effects. In addition, both Ki67 expression and CRT exposure in mice tumor tissue samples in S4-treated group and control group were assessed by immunohistochemistry. (Fig. 5B) shows both Ki67 staining and the CRT exposure was evidently observed in tumor samples of mice treated with S4 at either dose.

Discussion

In the present study, we provide evidence that the CAIX inhibitor S4 suppresses the growth of glioma cell in vitro and in vivo. Of note, we demonstrate that S4 triggers the expression of ICD markers in glioma cells via the ER stress pathway, indicating that S4 might be a novel ICD inducer. These findings merit further investigation to explore how S4 may be of use in glioma treatment.

The main finding of our study is that the CAIX inhibitor S4 could trigger ICD in glioma cells. ICD has emerged as a key component of therapy-induced anti-tumor immunity. Increasing evidence shows the propensity to undergo ICD as a prognostic factor associated with longer survival in cancer patients in general including glioblastoma patients [31]. Several chemotherapeutic agents such as cyclophosphamide [32], and oxaliplatinum [33], have shown to induce ICD in glioma in vitro and in mouse models [4]. Our data indicates that the CAIX inhibitor S4 might be a novel ICD inducer at least in glioma cells. To understand the underlying mechanism, we performed RNA-seq analysis of differentially expressed genes of cells treated with S4 or mock-treated, and found that the ER stress pathway is robustly enriched among the deregulated signaling pathways. ER stress is mainly accompanied by three sensors: PERK- eIF2α axis, which is pathognomonic for ICD, activating transcription factor 6 (ATF6), and inositol-requiring 1 (IRE1). We observed the elevated eIF2a phosphorylation and increased XBP1 levels, both markers of ER stress, in S4-treated glioma cells. Notably, pharmacological inhibition of the PERK-

eIF2α axis reversed S4-triggered induction of ICD markers. It should be pointed out that eIF2alpha phosphorylation is also considered as a hallmark of immunogenic cell death [34]. Therefore our data supports a role of ER stress in S4-induced ICD. ER stress is known to play a pivotal role in eliciting ICD [35–37]. Our recent work showed that ER stress is involved in oncolytic Newcastle disease virus-induced ICD in melanoma cells [38]. Altogether, both our current and previous work further highlight the recognized notion that ER stress plays a major role in intracellular signaling pathways that induce ICD [35]. We further tested how ER stress regulates S4-triggered ICD in glioma cells. Based on our findings that, inhibition of autophagy reduces S4-induced ICD, while inhibition of PERK antagonizes S4-induced autophagy, we could infer that ER stress plays a role in S4-induced ICD at least in part via autophagy. One of the limitations of our work is that how S4 evokes the ER stress in glioma cells remains unknown. In addition, it should be pointed out that the finding that S4 triggers ICD is largely achieved in in vitro experiments, therefore further work is needed to examine the direct influence by S4-mediated ICD on the immune environment in glioma.

Conclusions

In conclusion, we show the CAIX inhibitor S4 as a novel ICD inducer in glioma cells. Our findings highlight a novel mechanism for the antitumor actions of the CAIX inhibitor S4 and warrant further investigation of S4-induced ICD in clinical application.

Declarations

Author contributions

S.M., H.P., and Y.Y. conceived and designed the experiments. S.M., and Y. Y. wrote the manuscript. F.L., J.C., H.X, J.W. and J.S. conducted cell proliferation, colony formation, spheroid formation and immunoblotting assays. K.F. conducted immunofluorescence assays and assembled Figs. J.C. and K.F. conducted animal experiments. C.X., Z.X. conducted annexin V/PI apoptosis assay. D.L. analyzed the data. All authors discussed the results, commented on the manuscript, and approved the final manuscript.

Funding

The authors gratefully acknowledge the financial support from the Liaoning Revitalization Talents Program (No. XLYC1902023 to H. P.) the Natural Science Foundation of Liaoning Province (No. 2020-ZLLH-37 to J. S.), the National Natural Science Foundation of China (Nos. 82173032 and U21A20422 to H. P.) and the Cultivation Fund of Natural Science Foundation of Liaoning Cancer Hospital & Institute (No. 2021-ZLLH-01 to H. X.).

Data availability

All data reported in this paper will be shared by the lead contact upon request.

Conflict of interest The authors report no competing interests.

Ethical approval All animal studies were carried out at Dalian Medical University Laboratory Animal Center, and conducted in accordance with the national guidelines for the care and use of laboratory animals with approval from the experimental animal ethics committee: Dalian Medical University.

References

1. Finch A, Solomou G, Wykes V, Pohl U, Bardella C, Watts C (2021) Advances in Research of Adult Gliomas. Int J Mol Sci 22(2). https://doi.org/10.3390/ijms22020924
2. Hodge JW, Garnett CT, Farsaci B, Palena C, Tsang KY, Ferrone S et al (2013) Chemotherapy-Induced Immunogenic Modulation of Tumor Cells Enhances Killing by Cytotoxic T Lymphocytes and Is Distinct from Immunogenic Cell Death. Int J Cancer 133(3):624–636. https://doi.org/10.1002/ijc.28070
3. Krysko DV, Garg AD, Kaczmarek A, Krysko O, Agostinis P, Vandenabeele P (2012) Immunogenic Cell Death and Damps in Cancer Therapy. Nat Rev Cancer 12(12):860–875. https://doi.org/10.1038/nrc3380
4. Decraene B, Yang Y, De Smet F, Garg AD, Agostinis P, De Vleeschouwer S (2022) Immunogenic Cell Death and Its Therapeutic or Prognostic Potential in High-Grade Glioma. Genes Immun 23(1):1–11. https://doi.org/10.1038/s41435-021-00161-5
5. Garg AD, More S, Rufo N, Mece O, Sassano ML, Agostinis P et al (2017) Trial Watch: Immunogenic Cell Death Induction by Anticancer Chemotherapeutics. Oncoimmunology 6(12):e1386829. https://doi.org/10.1080/2162402X.2017.1386829
6. Hossain DMS, Javaid S, Cai M, Zhang C, Sawant A, Hinton M et al (2018) Dinaciclib Induces Immunogenic Cell Death and Enhances Anti-Pd1-Mediated Tumor Suppression. J Clin Invest 128(2):644–654. https://doi.org/10.1172/JCI94586
7. Kroemer G, Galluzzi L, Zitvogel L (2013) Immunological Effects of Chemotherapy in Spontaneous Breast Cancers. Oncoimmunology 2(12):e27158. https://doi.org/10.4161/onci.27158
8. Fucikova J, Moserova I, Truxova I, Hermanova I, Vancurova I, Partlova S et al (2014) High Hydrostatic Pressure Induces Immunogenic Cell Death in Human Tumor Cells. Int J Cancer 135(5):1165–1177. https://doi.org/10.1002/ijc.28766
9. D'Eliseo D, Manzi L, Velotti F (2013) Capsaicin as an Inducer of Damage-Associated Molecular Patterns (Damps) of Immunogenic Cell Death (Icd) in Human Bladder Cancer Cells. Cell Stress Chaperones 18(6):801–808. https://doi.org/10.1007/s12192-013-0422-2
10. Zitvogel L, Kepp O, Senovilla L, Menger L, Chaput N, Kroemer G (2010) Immunogenic Tumor Cell Death for Optimal Anticancer Therapy: The Calreticulin Exposure Pathway. Clin Cancer Res 16(12):3100–3104. https://doi.org/10.1158/1078-0432.CCR-09-2891
11. Pawaria S, Binder RJ (2011) Cd91-Dependent Programming of T-Helper Cell Responses Following Heat Shock Protein Immunization. Nat Commun 2:521. https://doi.org/10.1038/ncomms1524

12. Notomi S, Hisatomi T, Kanemaru T, Takeda A, Ikeda Y, Enaida H et al (2011) Critical Involvement of Extracellular Atp Acting on P2rx7 Purinergic Receptors in Photoreceptor Cell Death. Am J Pathol 179(6):2798–2809. https://doi.org/10.1016/j.ajpath.2011.08.035
13. Aymeric L, Apetoh L, Ghiringhelli F, Tesniere A, Martins I, Kroemer G et al (2010) Tumor Cell Death and Atp Release Prime Dendritic Cells and Efficient Anticancer Immunity. Cancer Res 70(3):855–858. https://doi.org/10.1158/0008-5472.CAN-09-3566
14. Swietach P, Vaughan-Jones RD, Harris AL (2007) Regulation of Tumor Ph and the Role of Carbonic Anhydrase 9. Cancer Metastasis Rev 26(2):299–310. https://doi.org/10.1007/s10555-007-9064-0
15. van Kuijk SJ, Yaromina A, Houben R, Niemans R, Lambin P, Dubois LJ (2016) Prognostic Significance of Carbonic Anhydrase Ix Expression in Cancer Patients: A Meta-Analysis. Front Oncol 6:69. https://doi.org/10.3389/fonc.2016.00069
16. Hedlund EE, McDonald PC, Nemirovsky O, Awrey S, Jensen LDE, Dedhar S (2019) Harnessing Induced Essentiality: Targeting Carbonic Anhydrase Ix and Angiogenesis Reduces Lung Metastasis of Triple Negative Breast Cancer Xenografts. Cancers (Basel) 11(7). https://doi.org/10.3390/cancers11071002
17. Chiaramonte N, Romanelli MN, Teodori E, Supuran CT (2018) Amino Acids as Building Blocks for Carbonic Anhydrase Inhibitors. Metabolites 8(2). https://doi.org/10.3390/metabo8020036
18. Federici C, Lugini L, Marino ML, Carta F, Iessi E, Azzarito T et al (2016) Lansoprazole and Carbonic Anhydrase Ix Inhibitors Sinergize against Human Melanoma Cells. J Enzyme Inhib Med Chem 31(sup1):119–125. https://doi.org/10.1080/14756366.2016.1177525
19. Gieling RG, Babur M, Mamnani L, Burrows N, Telfer BA, Carta F et al (2012) Antimetastatic Effect of Sulfamate Carbonic Anhydrase Ix Inhibitors in Breast Carcinoma Xenografts. J Med Chem 55(11):5591–5600. https://doi.org/10.1021/jm300529u
20. Winum JY, Carta F, Ward C, Mullen P, Harrison D, Langdon SP et al (2012) Ureido-Substituted Sulfamates Show Potent Carbonic Anhydrase Ix Inhibitory and Antiproliferative Activities against Breast Cancer Cell Lines. Bioorg Med Chem Lett 22(14):4681–4685. https://doi.org/10.1016/j.bmcl.2012.05.083
21. Meijer TW, Bussink J, Zatovicova M, Span PN, Lok J, Supuran CT et al (2014) Tumor Microenvironmental Changes Induced by the Sulfamate Carbonic Anhydrase Ix Inhibitor S4 in a Laryngeal Tumor Model. PLoS ONE 9(9):e108068. https://doi.org/10.1371/journal.pone.0108068
22. Ward C, Meehan J, Mullen P, Supuran C, Dixon JM, Thomas JS et al (2015) Evaluation of Carbonic Anhydrase Ix as a Therapeutic Target for Inhibition of Breast Cancer Invasion and Metastasis Using a Series of in Vitro Breast Cancer Models. Oncotarget 6(28):24856–24870. https://doi.org/10.18632/oncotarget.4498
23. Hektoen HH, Ree AH, Redalen KR, Flatmark K (2016) Sulfamate Inhibitor S4 Influences Carbonic Anhydrase Ix Ectodomain Shedding in Colorectal Carcinoma Cells. J Enzyme Inhib Med Chem 31(5):779–786. https://doi.org/10.3109/14756366.2015.1069286

24. van Kuijk SJ, Gieling RG, Niemans R, Lieuwes NG, Biemans R, Telfer BA et al (2016) The Sulfamate Small Molecule Caix Inhibitor S4 Modulates Doxorubicin Efficacy. PLoS ONE 11(8):e0161040. https://doi.org/10.1371/journal.pone.0161040
25. Bryant JL, Gieling RG, Meredith SL, Allen TJ, Walker L, Telfer BA et al (2018) Novel Carbonic Anhydrase Ix-Targeted Therapy Enhances the Anti-Tumour Effects of Cisplatin in Small Cell Lung Cancer. Int J Cancer 142(1):191–201. https://doi.org/10.1002/ijc.31042
26. Jiang K, Yao G, Hu L, Yan Y, Liu J, Shi J et al (2020) Mob2 Suppresses Gbm Cell Migration and Invasion Via Regulation of Fak/Akt and Camp/Pka Signaling. Cell Death Dis 11(4):230. https://doi.org/10.1038/s41419-020-2381-8
27. Sukkurwala AQ, Adjemian S, Senovilla L, Michaud M, Spaggiari S, Vacchelli E et al (2014) Screening of Novel Immunogenic Cell Death Inducers within the Nci Mechanistic Diversity Set. Oncoimmunology 3:e28473. https://doi.org/10.4161/onci.28473
28. Garg AD, Dudek AM, Ferreira GB, Verfaillie T, Vandenabeele P, Krysko DV et al (2013) Ros-Induced Autophagy in Cancer Cells Assists in Evasion from Determinants of Immunogenic Cell Death. Autophagy 9(9):1292–1307. https://doi.org/10.4161/auto.25399
29. Inoue H, Tani K (2014) Multimodal Immunogenic Cancer Cell Death as a Consequence of Anticancer Cytotoxic Treatments. Cell Death Differ 21(1):39–49. https://doi.org/10.1038/cdd.2013.84
30. Werthmoller N, Frey B, Wunderlich R, Fietkau R, Gaipl US (2015) Modulation of Radiochemoimmunotherapy-Induced B16 Melanoma Cell Death by the Pan-Caspase Inhibitor Zvad-Fmk Induces Anti-Tumor Immunity in a Hmgb1-, Nucleotide- and T-Cell-Dependent Manner. Cell Death Dis 6:e1761. https://doi.org/10.1038/cddis.2015.129
31. Fucikova J, Moserova I, Urbanova L, Bezu L, Kepp O, Cremer I et al (2015) Prognostic and Predictive Value of Damps and Damp-Associated Processes in Cancer. Front Immunol 6:402. https://doi.org/10.3389/fimmu.2015.00402
32. Du B, Waxman DJ (2020) Medium Dose Intermittent Cyclophosphamide Induces Immunogenic Cell Death and Cancer Cell Autonomous Type I Interferon Production in Glioma Models. Cancer Lett 470:170–180. https://doi.org/10.1016/j.canlet.2019.11.025
33. Roberts NB, Alqazzaz A, Hwang JR, Qi X, Keegan AD, Kim AJ et al (2018) Oxaliplatin Disrupts Pathological Features of Glioma Cells and Associated Macrophages Independent of Apoptosis Induction. J Neurooncol 140(3):497–507. https://doi.org/10.1007/s11060-018-2979-1
34. Bezu L, Sauvat A, Humeau J, Leduc M, Kepp O, Kroemer G (2018) Eif2alpha Phosphorylation: A Hallmark of Immunogenic Cell Death. Oncoimmunology 7(6):e1431089. https://doi.org/10.1080/2162402X.2018.1431089
35. Kepp O, Menger L, Vacchelli E, Locher C, Adjemian S, Yamazaki T et al (2013) Crosstalk between Er Stress and Immunogenic Cell Death. Cytokine Growth Factor Rev 24(4):311–318. https://doi.org/10.1016/j.cytogfr.2013.05.001
36. Sagar V, Vatapalli R, Lysy B, Pamarthy S, Anker JF, Rodriguez Y et al (2019) Ephb4 Inhibition Activates Er Stress to Promote Immunogenic Cell Death of Prostate Cancer Cells. Cell Death Dis

10(11):801. https://doi.org/10.1038/s41419-019-2042-y

37. Li X, Zheng J, Chen S, Meng FD, Ning J, Sun SL (2021) Oleandrin, a Cardiac Glycoside, Induces Immunogenic Cell Death Via the Perk/Elf2alpha/Atf4/Chop Pathway in Breast Cancer. Cell Death Dis 12(4):314. https://doi.org/10.1038/s41419-021-03605-y
38. Shao X, Wang X, Guo X, Jiang K, Ye T, Chen J et al (2019) Stat3 Contributes to Oncolytic Newcastle Disease Virus-Induced Immunogenic Cell Death in Melanoma Cells. Front Oncol 9:436. https://doi.org/10.3389/fonc.2019.00436

Figures

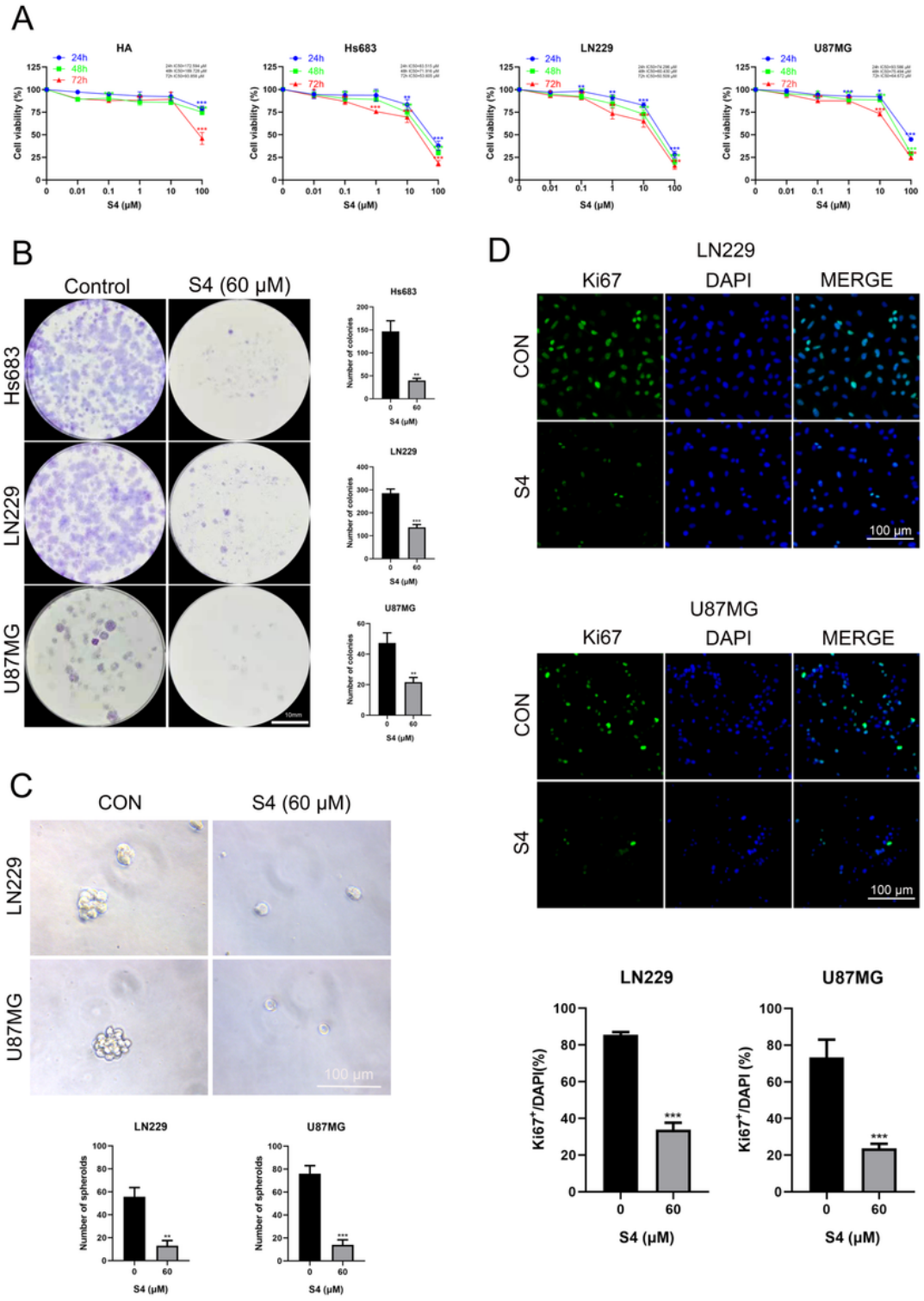

Figure 1

S4 decreases glioma cell viability. **(A)** HA, Hs683, LN229, and U87MG cells were vehicle-treated or treated with varying concentrations of S4 (0.01,0.1,1, 10, 100 μM) for 24, 48, 72 h respectively. Cell growth was determined using the CCK8 assay. **(B)** Cells (Hs683, LN229, and U87MG) were vehicle-treated or treated with 60 μM S4 and cultured in complete media for 14 days for colony formation analysis. **(C)** LN229 and U87MG cells cultured in 3D medium were treated with DMSO or 60 μM S4 for 12 days and examined for

the spheroid formation. (Scale bar = 100μm). **(D)** LN229 and U87MG cells were treated with DMSO or 60 μM S4, then assessed by immunofluorescence staining with ki67 or DAPI. (Scale bar = 100μm). The above experiments were performed three times. (*$P < 0.05$, **$P < 0.01$, ***$P < 0.001$).

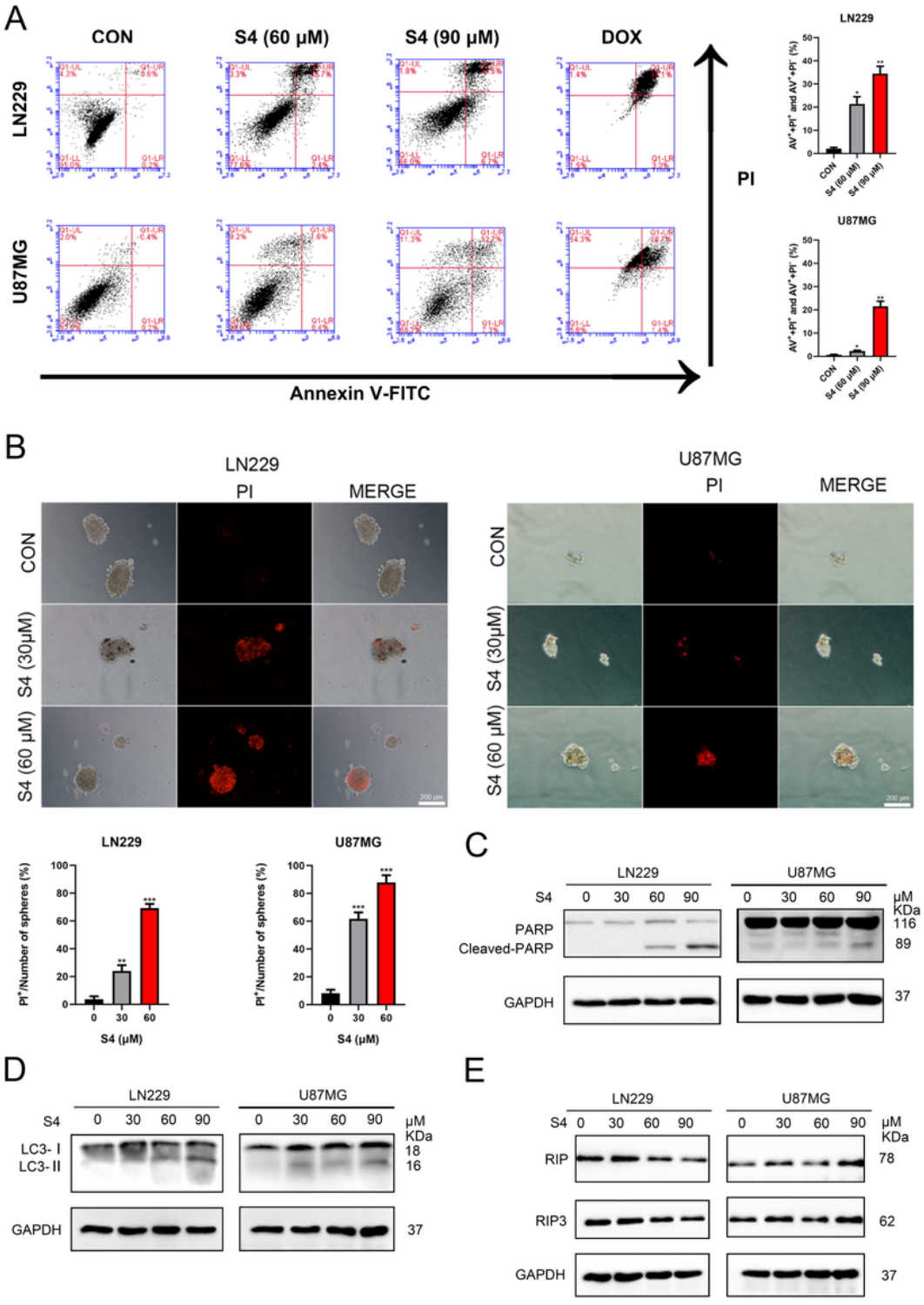

Figure 2

S4 induces glioma cell death. **(A)** LN229 and U87MG cells were treated with DMSO or S4 (60, 90 μM) for 24 h, stained with annexinV-FITC/PI. Cell death was assayed by flow cytometry. 5 μM concentration of Doxorubicin was taken as a positive control. **(B)** Spheroids were treated with DMSO or S4(30, 60 μM), stained with PI at 24 h and imaged under phase contrast and red fluorescence microscopy (scale bar = 200 μm). **(C-E)** LN229 and U87MG cells were treated with S4 (0, 30, 60, 90 μM) for 24 h, the relative expression of cleaved-PARP, LC3, RIP and RIP3 was determined by immunoblot analysis. GAPDH was used as a loading control. Experiments were performed three times. (*$P < 0.05$, **$P < 0.01$, ***$P < 0.001$).

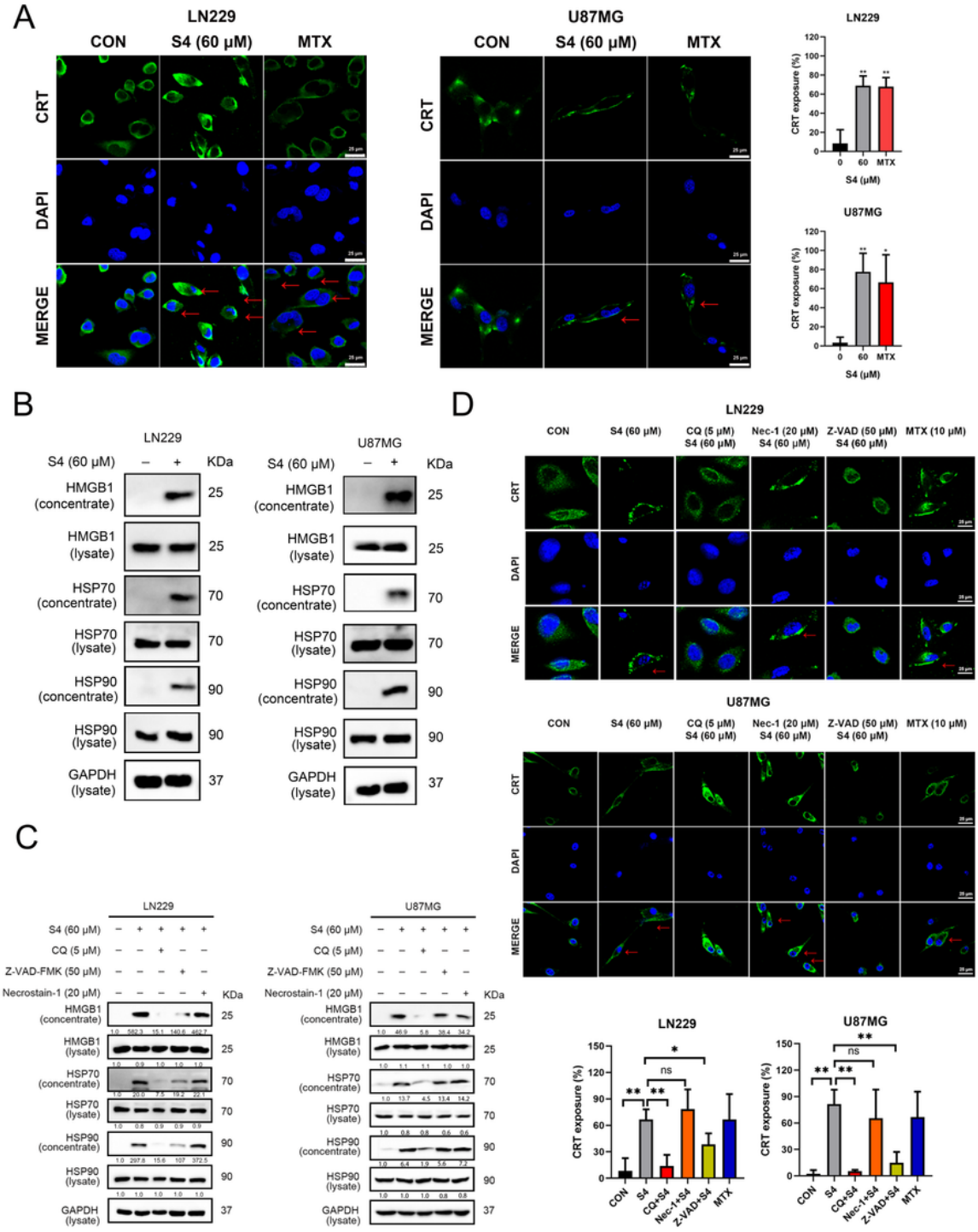

Figure 3

Autophagy and apoptosis are involved in S4-induced immunogenic cell death in glioma cells. **(A)** LN229 and U87MG cells were treated with DMSO or without S4 (60 μM) for 24 h, then stained with an anti-CRT antibody (Green). DAPI was used for nuclear staining (blue). The exposure of calreticulin (CRT) was assessed by confocal imaging. Mitoxantrine (MTX) was used as a positive control. ImageJ software was used to calculate the percentage of CRT positive area (**p < 0.01). Arrowheads indicate positive area. Images are representative of three independent experiments. (scale bar = 25 μm). **(B)** LN229 and U87MG cells were treated as in (A), cell lysates were collected and concentrated. HMGB1 and HSP70/90 expression were measured by immunoblot (IB) analysis. GAPDH was used as a loading control. (**C**) LN229 and U87MG cells were pre-treated with either Z-VAD-FMK (50 μM), or chloroquine (CQ, 5 μM), or Necrostain-1 (20 μM), following treatment with S4 (60 μM) for 24h, then cell lysates and cell-free supernatants (concentrated) were collected. HMGB1 and HSP70/90 levels were measured by IB analysis. GAPDH was used as a loading control. (**D**) Exposure of CRT (green) was assessed by immunofluorescence staining. DAPI was used for nuclear staining (blue). MTX was used as a positive control. Arrowheads indicate positive area. (scale bar = 25 μm). The above experiments were performed three times.(*P < 0.05, **P < 0.01).

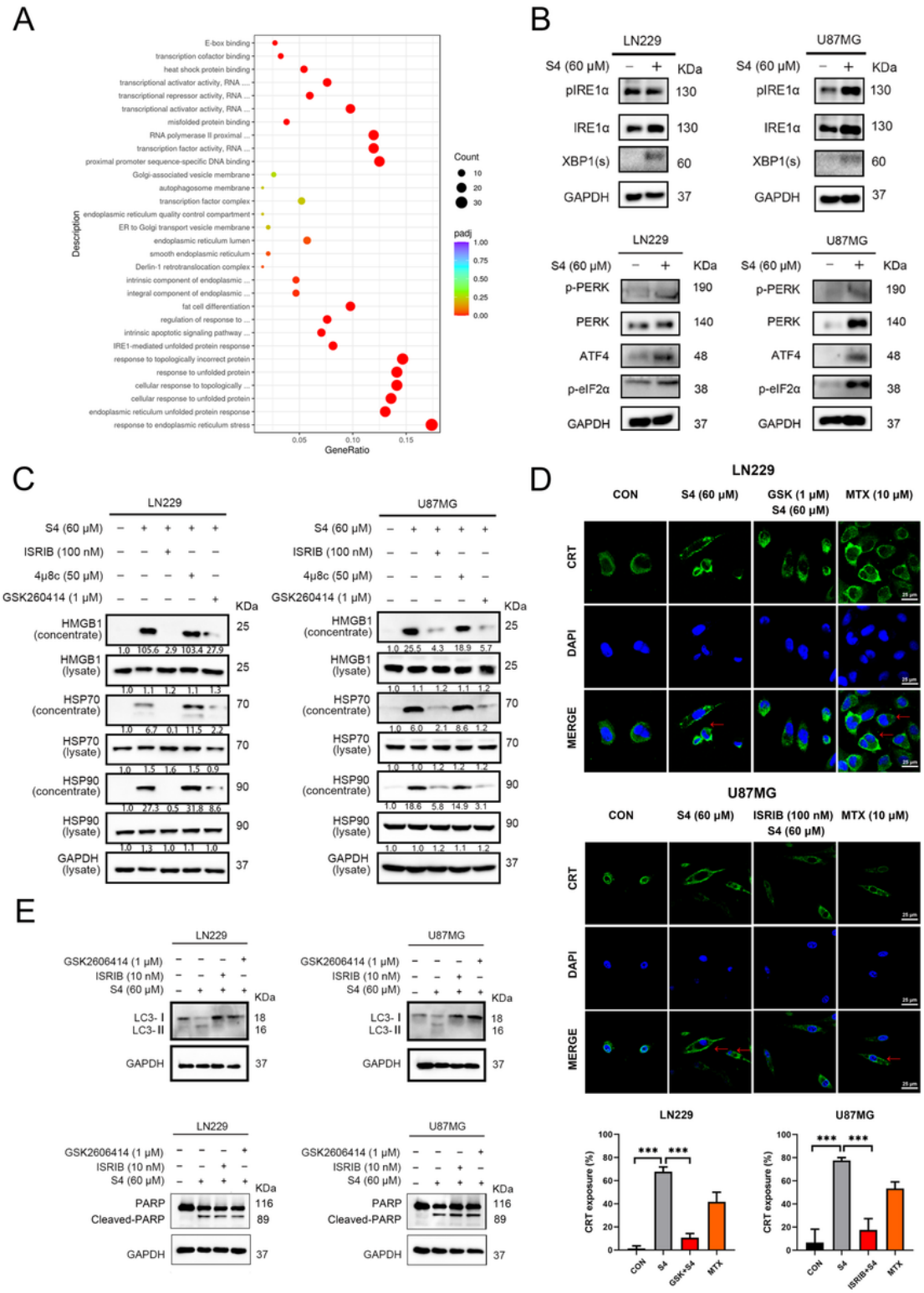

Figure 4

PERK pathway contributes to S4-induced immunogenic cell death in glioma cells. **(A)** LN229 cells treated with S4 (60 μM) or DMSO for 12h were collected for transcriptome sequencing. Differentially expressed genes were analyzed by gene ontology. **(B)** Immunoblot (IB) analysis was performed to detect the action of the PERK pathway related proteins P-perk, ATF4, P-elf2α, and the IRE1α-XBP1 pathway related proteins pIRE1α, IRE1α, XBP1(s). **(C)** LN229 and U87MG cells were treated either IRE1α -xbp1 pathway inhibitor

4μ8C (50 μM), or PERK pathway inhibitors GSK2606414 (1 μM) and ISRIB (100 nM) with S4 (60 μM) for 24 h and the expression of HMGB1 and HSP70/90 was measured by IB analysis. **(D and E)** LN229 and U87MG cells were treated with S4 (60 μM) and GSK2606414 or ISRIB respectively, the CRT exposure was detected by confocal microscopy (scale bar = 25 μm), expression of LC3II and Cleaved-PARP was examined by IB analysis. Arrowheads indicate positive area. The above experiments were performed three times.(*P < 0.05, **P < 0.01, ***P < 0.001).

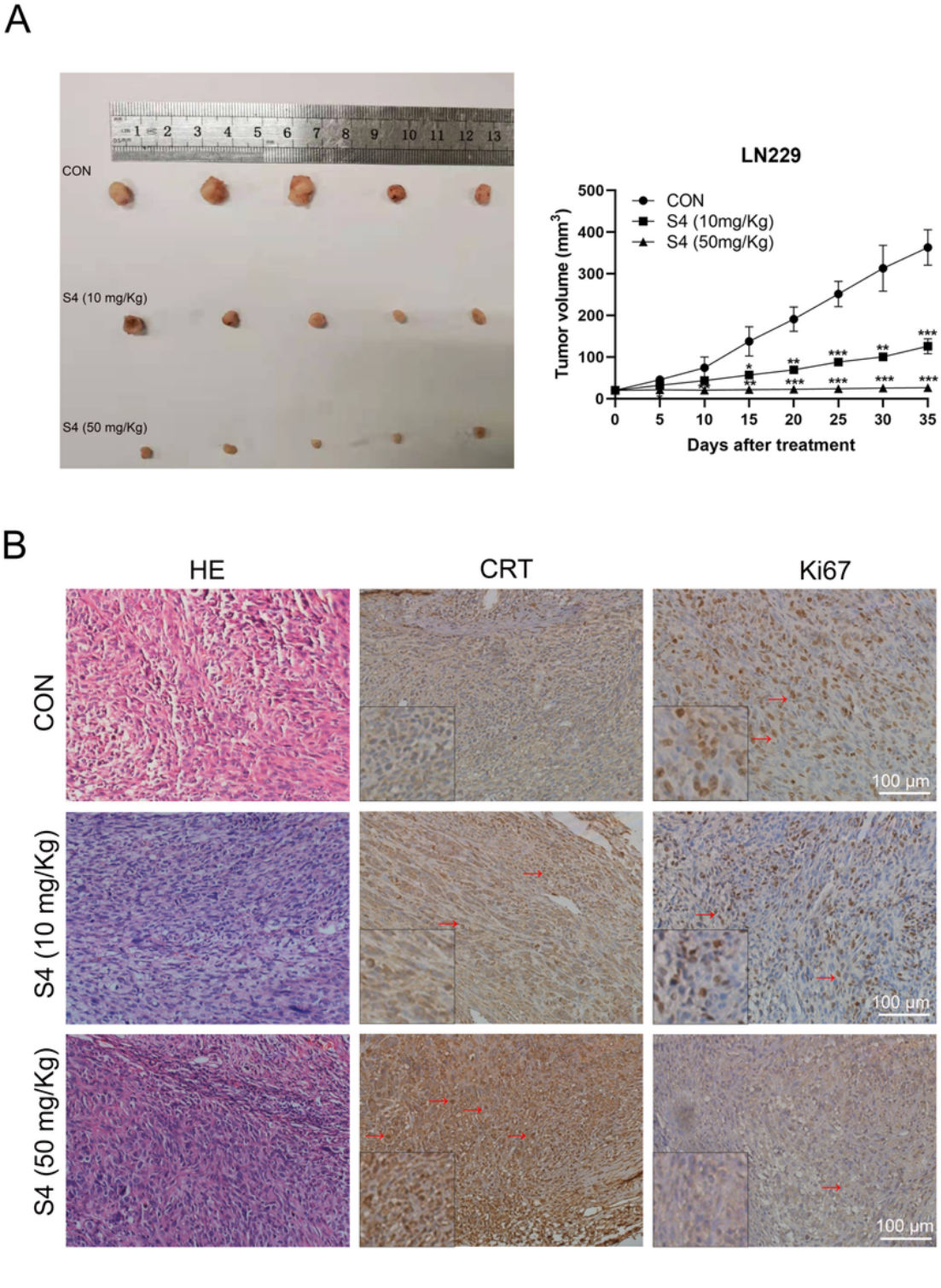

Figure 5

S4 reduces glioma growth in mice models and induces exposure of CRT. **(A)** LN229 cells were injected subcutaneously into the right flanks of mice to establish tumors. When tumors reached approximately 20 mm^3, mice received an intratumoral injection of either DMSO, or S4 (10mg/Kg, 50mg/Kg respectively) every three days, n=5 in each group. Tumor volumes were measured at 5-day intervals for 35 days after injections and expressed as the Mean ± SD. Tumor volume-time curves to show any differences in tumor regression. **(B)** Hematoxylin and eosin (H&E) was used to examine tumor tissues, and immunohistochemistry assay was performed to detect CRT and Ki67 respectively. Arrowheads indicate positive area. (scale bar = 100 μm). (*P < 0.05, **P < 0.01, ***P < 0.001).